Three-Dimensional Flow Characteristics within the Scour Hole around Circular Uniform and Compound Piers

Ashish Kumar[1] and Umesh C. Kothyari[2]

Abstract: The experimental observations are presented on flow patterns and turbulence characteristics measured by an acoustic Doppler velocimeter within the developing (transient stage) scour hole around circular uniform and compound piers. Four series of experimental runs were conducted under the clear-water approach flow conditions. One experimental run was conducted around a uniform circular pier of diameter 114 mm, whereas the other three runs were conducted around a circular compound pier of diameter 114 mm and footing diameter 210 mm. In the series with a circular compound pier, the top surface of the footing was placed at three different elevations with respect to the general level of the channel bed, i.e., above the bed level, at the bed level, and below the level of the channel bed. Detailed measurements are presented on components of time-averaged velocity, turbulence intensity, and Reynolds shear stress around the pier in radial planes at 0°, 90°, and 180° from the flow axis. Flow structure around a circular compound pier in the presence of a scour hole was compared with flow structure similarly observed around a circular uniform pier by utilizing the observations made in radial planes at 0°, 30°, 60°, 90°, 120°, 150°, and 180° from flow axis. Diameter of the principal vortex upstream of the compound pier, when top surface of the footing is above the general level of the channel bed was 1.11 times as large as that for the circular uniform pier. However, size of the principal vortex is 0.85 times its size for the uniform pier, whereas the top surface of the footing was below the channel bed level. The components of turbulence intensities and Reynolds shear stress profiles in different radial planes are also compared around each of the pier models. **DOI: [10.1061/(ASCE)HY.1943-7900 .0000527](.)**. © *2012 American Society of Civil Engineers.*

CE Database subject headings: Piers; Scour; Three-dimensional flow; Turbulence.

Author keywords: Acoustic Doppler velocimeter; Compound pier; Scour; Three-dimensional flow; Turbulence; Uniform pier.

Introduction

A considerable amount of literature exists on the topic of bridge scour, and large numbers of empirical and semiempirical relations were developed in recent years for computation of scour depth around piers of different geometries (Kothyari et al. 2007). The predictions of scour depths by the existing models may not always be realistic. A lack of understanding of the flow pattern around bridge piers is the main reason for such a problem. Therefore investigations were conducted in the past for study of the scouring process and flow structure around circular uniform bridge piers by Melville and Raudkivi (1977); Dey et al. (1995); Ahmed and Rajaratnam (1998), Graf and Istiarto (2002), Muzzammil and Gangadhariah (2003), Dey and Raikar (2007), among others.

The actual bridge piers, however, are built in a variety of geometries and most of these have nonuniform cross sections along their height (Melville and Raudkivi 1996). Circular compound pier foundations are mostly adopted in bridges across the alluvial plains of Ganaga-Yamuna and Brahmputra Rivers in the Indian subcontinent. The circular pier resting on larger diameter circular footing, also called a well or caisson, is a circular compound pier. In the case

of the compound piers, geometry of the piers is not uniform along their height, therefore compared with the uniform piers, the flow structure around them becomes more complicated even in the case of geometries that are circular in plan. The flow and turbulence characteristics around circular compound bridge piers in the presence of a developing scour hole have not been studied.

Simulation of flow structure in scour hole around circular uniform pier is reported by Ali et al. (1997), Richardson and Pancheng (1998), Olsen and Kjellesnig (1998), and Salaheldin et al. (2004), etc. However, an exhaustively complete comparison is yet to be made between the mathematically simulated and the experimentally observed results on flow structure around bridge piers because of a lack of detailed data.

In the present study, a carefully controlled set of experiments was carried out to better understand the flow structure and the turbulence characteristics around a uniform circular pier and a compound circular pier in the presence of a scour hole. A comparative study between these flow structures is presented. Fig. 1 shows the definition diagram of a circular compound bridge pier where b = the diameter of the pier; b_* = the diameter of foundation or footing; h = the depth of flow; and Y = depth of the top surface of the footing (foundation) below the initial bed level of the channel. It is expected that the new observations on flow structure presented herein shall be useful in modeling the process of scour around uniform and compound piers. These shall also be useful in further developing the measures for scour protection around these structures.

Experimental Setup

The experiments were conducted in a 30.0-m long, 1.0-m wide rectangular channel. The working section was located 12.0 m

---

[1]Assistant Professor, Dept. of Civil Engineering, Jaypee Univ. of Information Technology, Waknaghat, Solan (H.P.), India (corresponding author). E-mail: ashish.fce@juit.ac.in; rohilpce@rediffmail.com

[2]Professor, Dept. of Civil Engineering, Indian Institute of Technology, Roorkee, India.
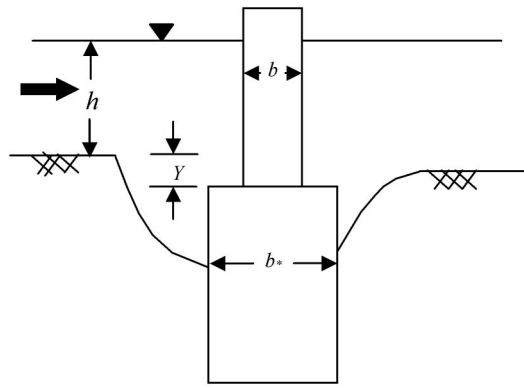
Fig. 1. Definition diagram of circular compound bridge pier

downstream of the flume entrance, with the dimensions length = 3.0 m, depth = 0.6 m, and width = 1.0 m. The working section was filled with uniform cohesionless material (sand) with a median size $d_{50} = 0.4$ mm.

Four experiments were performed in which a scour hole was allowed to develop up to the semiequilibrium stage before the observations were made using an acoustic Doppler velocimeter (ADV). Two pier models were used for the experimentation. One uniform circular pier, named UPSH with a diameter equal to 114 mm and another circular compound bridge pier with a pier diameter equal to 114 mm and well diameter equal to 210 mm. In circular compound pier runs, the top surface of footing was kept at three different elevations with respect to original bed level of the channel, i.e., above the bed level ($Y = -b_*/10$) for run NUPSH 2, at the bed level ($Y = 0$) for run NUPSH 1, and below the bed level ($Y = b_*/10$) for run NUPSH 3. During the experiments, a discharge Q of 0.045 m^3/s and flow depth h of 160 mm was maintained. This yielded an average approach flow velocity U_∞ equal to

0.28 m/s ($u_*/u_{*c} \approx 0.92$) at 2.0 m upstream of the pier, where effect of the pier on the flow was considered to be negligible. Here, u_* is shear velocity of approach flow and u_{*c} is critical shear velocity determined as per Shields criterion.

In each of the experimental runs, the pier model was installed vertically in the middle of the test section, and the aforementioned flow condition was established. The temporal variation of scour depth was also monitored (albeit not analyzed here) at the upstream nose of the pier for all four experimental runs. Scour depth develops asymptotically with time. It is, however, well known that scour development is rapid during the initial stages and becomes slow after a few hours of scour activity. Before making observations for the flow field, the pier scour was allowed to progress for a period of 7 h in all the experiments. The data collected in the present study, therefore, correspond to the condition of developing (transient) scour hole.

The maximum scour depth d_s measured at the upstream nose of the pier at the end of experimental run was 139, 144, 149, and 101 mm, respectively, for runs UPSH, NUPSH 1, NUPSH 2, and NUPSH 3. Contours of scour depth for these runs are shown in the Fig. 2, which quantifies the extent of scour in the different experimental runs. Fig. 3 shows the observed temporal variation of scour depth for all runs. Here, d_{st} is the depth of scour below the initial bed level at time t. The maximum depth of scour formed over the duration of experimental run was compared with equilibrium scour depth d_{se} determined as per the method of Melville and Chiew (1999). It was noted that the maximum depth of scour developed in present runs varied from 32.3% to 52.4% of the equilibrium depth of scour. Hence the flow structure studied in the present runs is considered to correspond to the developing (transient) scour condition.

Before making observations for the flow field, the geometry of evolved scour hole around the pier was stabilized after the water was completely drained from it by using a light solution of cement that was sprayed over the surface of the scour hole, and the
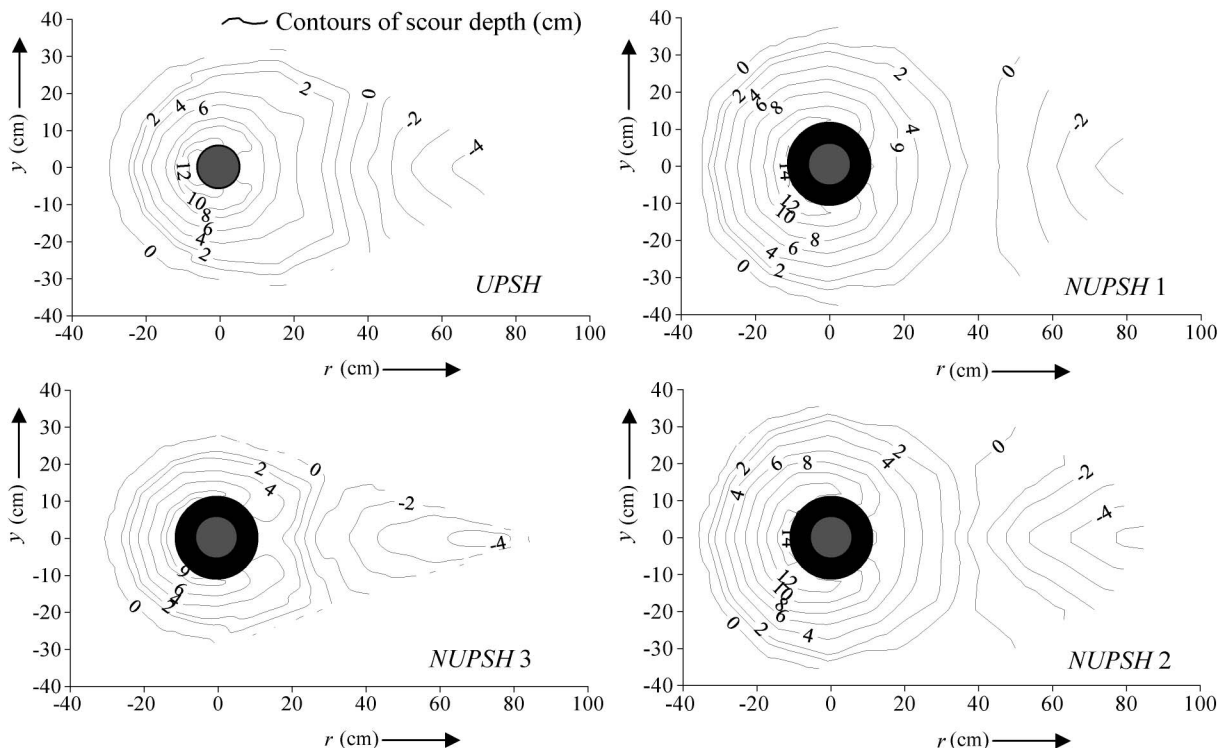
Fig. 2. Contours of scour depths for the uniform circular pier run and compound circular pier runs
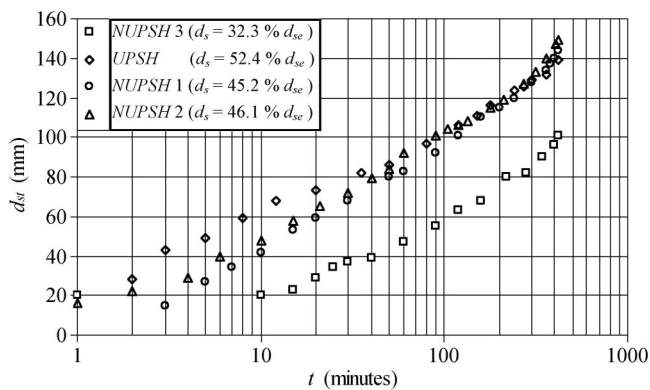
Fig. 3. Temporal variation of scour depth for all experimental runs (d_{se}-equilibrium scour depth computed by the method of Melville and Chiew [1999])

Fig. 4. Measurement stations around the piers (all dimensions are in mm)

sediment deposited downstream of the pier. Following Dey and Barbhuiya ([2005]) it is considered that there may be a slight change in the bed roughness attributable to spraying the light solution of cement on the surfaces of the scour hole, and flow close to the bed may thus be altered. However, the basic flow structure around the pier will not alter.

The velocity measurements were made using Nortek ADV at a frequency of 25 Hz in a small sampling volume (approximately 0.085 cm^3) that was 50 mm away from the sensing elements. The sample volume can be described roughly as a cylinder with a diameter approximately 6 mm and a height of 3 mm. Following Dey and Raikar ([2007]), the nearest vertical distance of velocity measurements from the bed surface maintained was 4 mm. Measurements were taken by using the down-looking probe and upward-looking probe of the ADV.

The measurements were taken at any particular point for 2-min to 4-min duration to ensure that observations become stationary. Each time series on velocity components was edited for a minimum signal-to-noise ratio of 17 and minimum correlation coefficient of 70%. The accuracy of velocity data collected by ADV was checked by the software WinADV developed by the United States Bureau of Reclamations, Water Resources Research Laboratory ([Wahl 2000]). The difference in variance with the nonfiltered signal was calculated. The maximum difference was found to be less than 3%, which assured the goodness of measurements.

After the geometry of the scour hole was stabilized for each run, the measurements for velocity components were made in vertical planes of symmetry, respectively, in radial planes at $\alpha = 0°$, $60°$, $90°$, $120°$, $150°$, and $180°$. Here, angle $\alpha = 0°$ corresponded to the central line of the flow on the upstream part of the pier. Fig. 4 shows the positions of such measurement stations around the circular pier. Velocity distributions along eight vertical profiles located at different radial distances (r) from the center of the pier, i.e., $r = 100$, 140, 170, 200, 250, 300, 350, and 400 mm, were observed in each of the radial planes. Vertical distributions of the time-averaged velocity components (u, v, w) were obtained at the measuring stations located at any observation point $P(r, \alpha, z)$; see Fig. 4. Here, z is the vertical distance from the channel bed. Along any vertical, measurement of velocity distributions were taken at an interval of 10 mm. Time-averaged velocity components (radial u_r, angular u_α, and vertical w) are defined in the cylindrical coordinate system (r, α, z), which is being used for velocity vector plotting. The data collected in the present study are given in Kumar ([2007]) and these data, along with results, are also listed in detail in Kumar ([2010]).
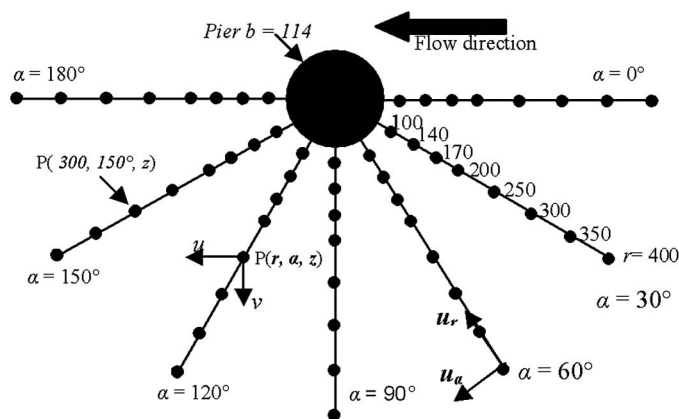
Flow Field around Circular Piers

The measurements of velocity, turbulence intensities ($\sqrt{\overline{u'u'}}$, $\sqrt{\overline{v'v'}}$, $\sqrt{\overline{w'w'}}$), and Reynolds shear stress ($\overline{u'w'}$, $\overline{v'w'}$) were made around each of the pier models at different vertical planes in radial directions having $\alpha = 0°$, $30°$, $60°$, $90°$, $120°$, $150°$, and $180°$ ([Kumar 2007]). Here, u' is the fluctuation of u component, v' is fluctuation of v component, and w' is fluctuation of w component of flow velocity. For each angle (α) and each radial distance (r), a comparative study on the flow structure around the circular uniform pier and the circular compound pier in the presence of the scour hole around them is conducted. However, discussions on time-averaged velocities, turbulence intensities, and Reynolds shear stress are given here only for data along the planes with $\alpha = 0°$, $90°$, and $180°$ because of the lack of space. The analysis is focused on the alteration caused in the flow structure by the combined effect of pier and position of the top surface of the footing with respect to the channel bed.

Measurements in the Plane at $\alpha = 0°$

Measurement of velocity data, turbulence intensities, and Reynolds shear stress are taken in radial direction $100 \leq r \leq 400$ mm, which covers the scoured region and some extent of the outer region beyond the scoured area.

Fig. 5 exhibits the comparison of u and w in the plane at $\alpha = 0°$ for all the runs. Close to the pier at $r/r_p = 1.75$ and in the upper region, profiles of u show an almost similar trend. Here r_p is radius of the pier. Value of u is reduced for run NUPSH 3. In the presence of a scour hole, the top surface of footing of the compound pier in the run NUPSH 3 would be exposed to the flow. Therefore, part of the vortex on the upstream of the pier shall be resting on the top surface of the footing, which is rigid. It, therefore, had the vortex supporting ability. The smaller value of u observed for run NUPSH 3 is attributed to the vortex supporting ability of the footing. The v component of velocity is almost negligible for all experimental runs in the entire region of flow.

Close to the pier at $r/r_p = 1.75$, the downward component w is higher for the UPSH run, whereas for other experimental runs w is smaller because of the presence of footing as the top rigid surface of footing did not allow the flow acceleration in the downward direction close to outer face of the pier. For $2.46 \leq r/r_p \leq 3.5$, in the scour hole region and below the general bed level ($z < 0$), the magnitude of w component is higher for run NUPSH 2 compared with run NUPSH 1. At $r/r_p = 2.46$, the maximum value of w for
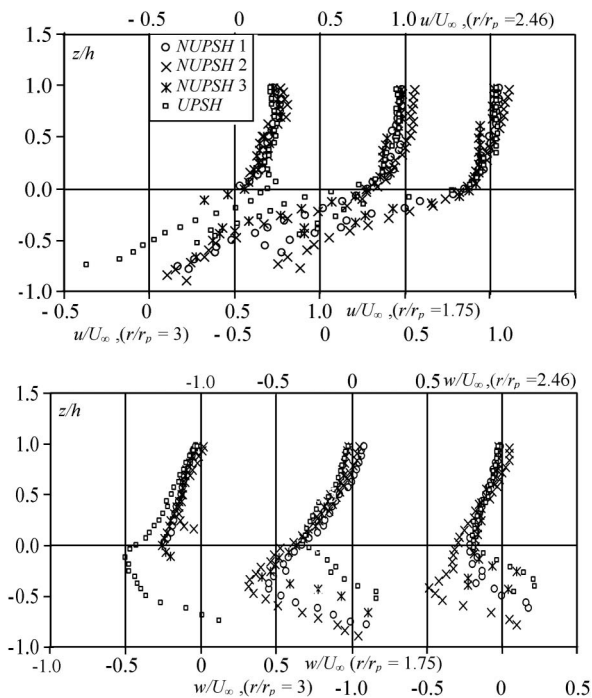
Fig. 5. Comparison of normalized u and w components of velocity of circular uniform pier run (UPSH) with the circular compound pier runs (NUPSH 1, NUPSH 2, and NUPSH 3) at plane $\alpha = 0°$

NUPSH 2 is equal to $-0.68\ U_\infty$, whereas in the case of the circular uniform pier, maximum value of w is noticed to be equal to $-0.5\ U_\infty$ at $r/r_p = 1.75$, i.e., close to the pier. Far away from the scour hole region the w component is negligible for all the runs. These observations indicate that the maximum value of w occurred at different values of r/r_p in runs NUPSH 2 and UPSH. This is attributed to the reason that in run NUPSH 2, the top surface of the footing is above the general level of channel bed and below the level of the water surface. Therefore, down flow would be affected in this run attributable to exposure of the footing to the flow.

Figs. 6(a)–6(c) represent the vertical distribution of turbulence intensities normalized by u_* for runs UPSH, NUPSH 1, NUPSH 2, and NUPSH 3. At $r/r_p = 5.26$, the vertical distribution of all the components of turbulence intensity for NUPSH runs is similar to those of the UPSH run. Within the scoured region, however, the distributions of data quantify the effect of the foundation geometry. Higher magnitude of turbulence intensity is observed within the scoured region and below the general bed level for NUPSH 2, which indicates that flow turbulence increases when footing top is exposed to the flow.

The vertical distribution of Reynolds shear stress for all the runs is given in Kumar (2007, 2012). Above the general bed level, the profiles of Reynolds shear stress components for NUPSH runs are similar to that for the UPSH run. However, the $\overline{u'w'}$ is dominant over $\overline{v'w'}$ component within the scoured region and below the general bed level. Beyond the extent of scour hole the shear stress component for all the runs has a value close to zero and hence not shown here.

The combined effect of the all the three components of the turbulence intensity can be better presented in terms of turbulent kinetic energy (k) of the flow, defined as:

$$k = \frac{1}{2}(\overline{u'u'} + \overline{v'v'} + \overline{w'w'}) \tag{1}$$

The vertical distribution of k for the all the runs are given in details in Kumar (2010). In the upper region while $z > 0$, the data of k follow the same type of trend and show almost similar values for all the runs. Run NUPSH 2 had higher turbulent energy than all the other runs within the scour hole region. For all the runs of compound piers, the value k was noticed to be higher than that observed in UPSH run.

Measurements in the Plane at $\alpha = 90°$

The vertical distribution of u, v and w; comparison of $\sqrt{\overline{u'u'}}$, $\sqrt{\overline{v'v'}}$, $\sqrt{\overline{w'w'}}$; normalized $\overline{u'w'}$, $\overline{v'w'}$; and distribution of normalized k in the plane at $\alpha = 90°$ are also shown in Kumar (2010). These figures revealed that close to the pier, the magnitude of u component was higher for run NUPSH 2. Away from the scoured region while $r/r_p > 3.5$, the u, v, and w component in the upper zone have almost the same values and hence the effect of relative location of the top surface of the footing on these was negligible. All three components of velocity have relatively larger magnitude within the scoured region for runs NUPSH 2 and NUPSH 1 than that for runs NUPSH 3 and UPSH.

The w component is considerably reduced in this plane for the NUPSH 3 run. However, compared with its value for UPSH run, the w component is higher for runs NUPSH 2 and NUPSH 1.

The profiles of all the three components of turbulence intensity and components of Reynolds shear stress show a repetitive trend. However, values of the turbulence intensity and Reynolds shear stress were higher for runs NUPSH 1 and NUPSH 2. The magnitude of k for all the runs is relatively higher here than those in the planes at $\alpha = 0°$. The increased magnitude of k indicates that this plane constitutes the zone of high turbulent mixing. Thus, the magnitude of k is noticed to increase as the flow moved toward the pier downstream.

Measurements in the Plane at $\alpha = 180°$

Figs. 7(a)–7(c) illustrate the comparison of normalized components of u, v, and w for run UPSH, with those for runs NUPSH 1, NUPSH 2, and NUPSH 3 at $\alpha = 180°$. The reversal of flow just near the pier is evident in these figures. In the wake region, the magnitude of u was higher for run UPSH than for runs NUPSH. The v component varied about its mean value along the entire depth of flow, whereas the w component is positive over the entire depth of flow in this plane. However, for NUPSH runs, flow reversal occurs at the base of the footing. Approaching the pier, the peak of w occurs near the general bed level in all the runs. Further downstream of the pier the peak of velocity profiles moves toward the water surface. Close to the pier, however, the w component is small in magnitude for run NUPSH 3.

Figs. 8(a)–8(c) depict the comparison of normalized components of turbulence intensities in run UPSH with NUPSH runs in the plane having $\alpha = 180°$. Close to the pier, no conclusive trend could be identified in these data. However, $\sqrt{\overline{v'v'}}$ was noticed to be dominant over the other two components in all the runs. The intensity of turbulence is higher in run NUPSH 2. Magnitude of intensity of turbulence is observed in decreasing order for NUPSH 1, UPSH, and NUPSH 3.

The comparison of normalized $\overline{u'w'}$, $\overline{v'w'}$ and distribution of normalized k in the plane at $\alpha = 180°$ were also plotted for all the runs (Kumar 2010). The profiles of $\overline{v'w'}$ showed positive and negative value along the depth of flow for all the runs, thus indicating the transverse momentum exchange in the wake region. Further downstream of the pier, the decrease in intensity of turbulence is evident from these figures. The magnitude of k was highest for run NUPSH 2. The magnitude of k decreases toward the water surface. The profiles of k downstream of the pier showed no

JOURNAL OF HYDRAULIC ENGINEERING © ASCE / MAY 2012 / **423**
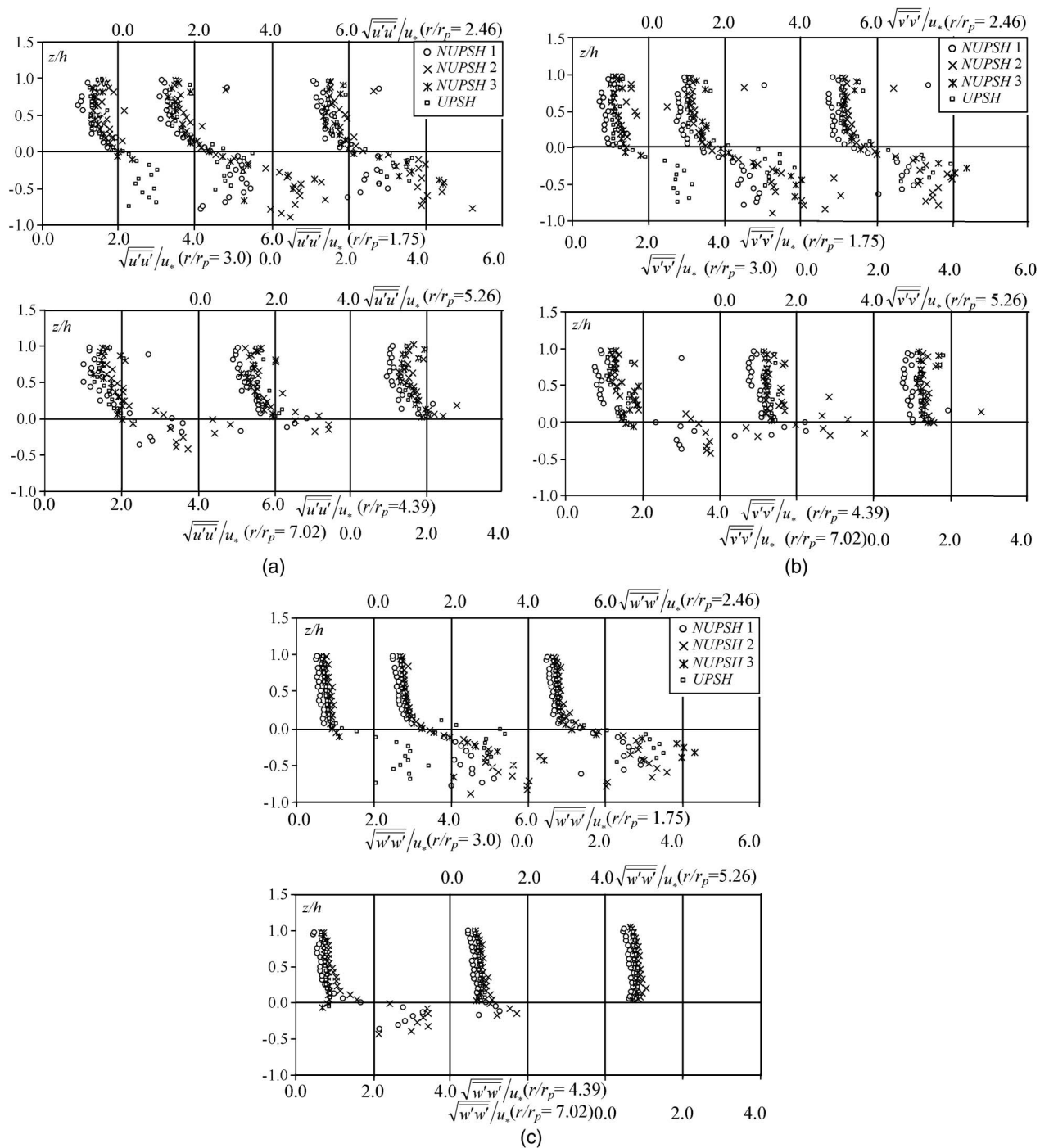
Fig. 6. (a) Comparison of normalized $\sqrt{\overline{u'u'}}$ component of turbulence intensity of circular uniform pier run (UPSH) with the circular compound pier runs (NUPSH 1, NUPSH 2, and NUPSH 3) at plane $\alpha = 0°$; (b) comparison of normalized $\sqrt{\overline{v'v'}}$ component of turbulence intensity of circular uniform pier run (UPSH) with the circular compound pier runs (NUPSH 1, NUPSH 2, and NUPSH 3) at plane $\alpha = 0°$; (c) comparison of normalized $\sqrt{\overline{w'w'}}$ component of turbulence intensity of circular uniform pier run (UPSH) with the circular compound pier runs (NUPSH 1, NUPSH 2, and NUPSH 3) at plane $\alpha = 0°$

conclusive trend but further downstream from the pier, these profiles become comparable.

Flow Pattern around the Circular Uniform and Compound Piers

Fig. 9 shows the complete picture of measured velocity field in the scoured area in the planes upstream and downstream of all the runs.

The rotating flow is inside the scoured area at $\alpha = 0°$, which is commonly known as the principal vortex of the horseshoe vortex system, whereas the downward flow is observed in the upstream face close to the pier and near the base of scoured area for all the runs.

The velocity vector field measured by ADV upstream of each of the runs was used for deciding the observed size of the principal vortex. The velocity vectors bending downward and clockwise

424 / JOURNAL OF HYDRAULIC ENGINEERING © ASCE / MAY 2012
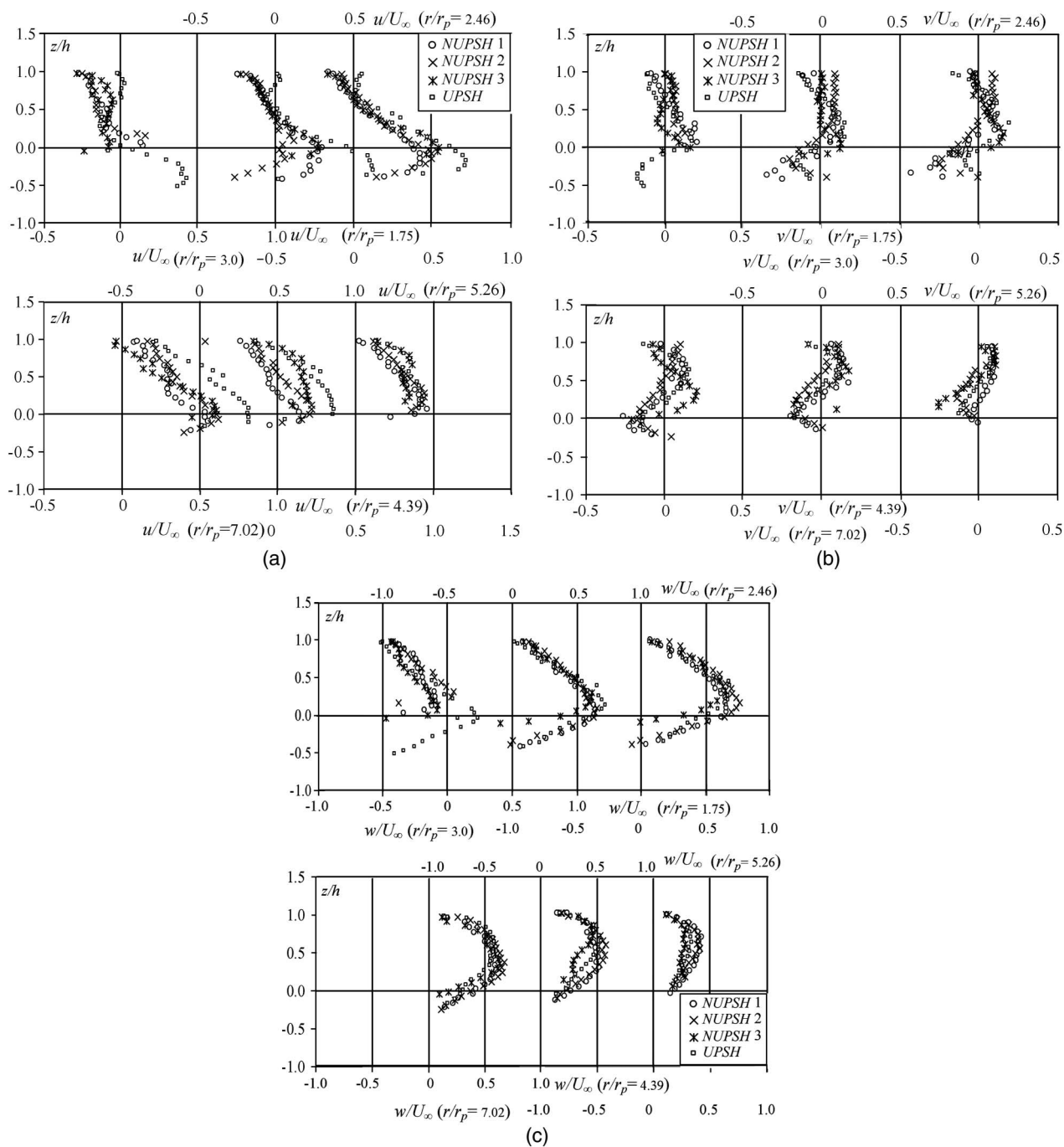
Fig. 7. (a) Comparison of normalized u component of velocity of circular uniform pier run (UPSH) with the circular compound pier runs (NUPSH 1, NUPSH 2, and NUPSH 3) at plan $\alpha = 180°$; (b) comparison of normalized v component of velocity of circular uniform pier run (UPSH) with the circular compound pier runs (NUPSH 1, NUPSH 2, and NUPSH 3) at plan $\alpha = 180°$; (c) comparison of normalized w component of velocity of circular uniform pier run (UPSH) with the circular compound pier runs (NUPSH 1, NUPSH 2, and NUPSH 3) at plan $\alpha = 180°$

from the horizontal and having an inclination more than 10° with the horizontal were included inside the upper periphery of the vortex. The cross-sectional area of the principal vortex is considered to be equal to the area of thus formed vortex structure. The diameter of the principal vortex was determined for each of the runs. Thus determined principal vortex for run NUPSH 2 was 11% larger in size than for run UPSH. This is attributed to the exposure of a part of footing to the flow. Similarly, the diameter of principal vortex for run NUPSH 3 was 0.85 times its size for run UPSH. As $Y = b_*/10$, for run NUPSH 3 the principal vortex, therefore, rested on the top rigid surface of the footing, which has been termed as vortex

supporting ability of the footing. A smaller size of principal vortex and a less depth of scour was observed for run NUPSH 3 compared with the other runs (see Fig. 3) because of the vortex supporting ability of the footing in this run. Size of the principal vortex within the scour hole, however, mainly varied with depth of scour and position of footing top surface with respect to the channel bed level.

Downstream of the pier, reversal of flow toward the water surface is revealed from the velocity vector plots for all the runs. The feature of flow reversal gradually disappears while one moves further downstream from the pier. For all the compound pier runs, the flow pattern around the pier was similar in profile as for the run

JOURNAL OF HYDRAULIC ENGINEERING © ASCE / MAY 2012 / **425**

J. Hydraul. Eng., 2012, 138(5): 420-429
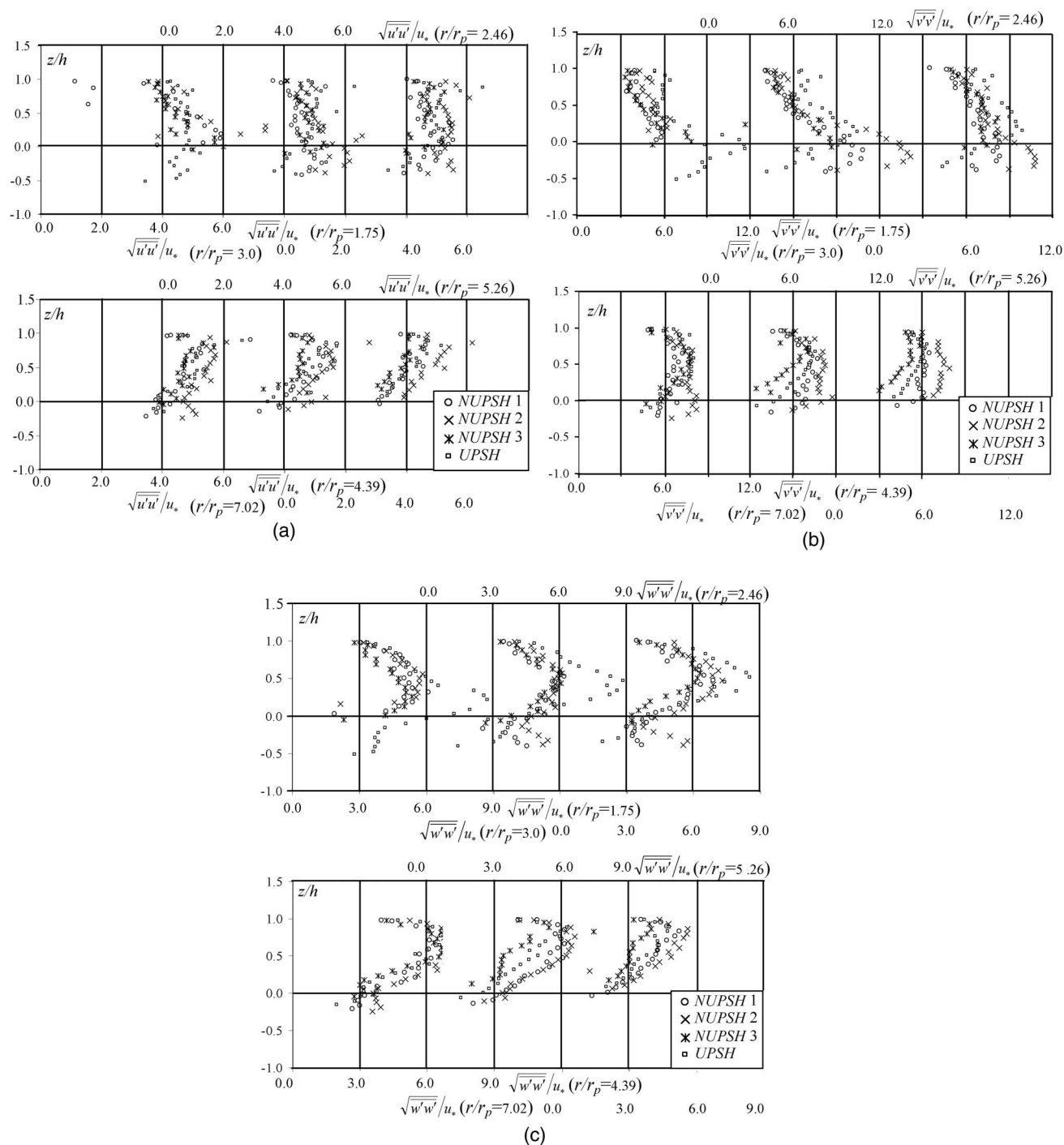
Fig. 8. (a) Comparison of normalized $\sqrt{\overline{u'u'}}$ component of turbulence intensity of circular uniform pier run (UPSH) with the circular compound pier runs (NUPSH 1, NUPSH 2, and NUPSH 3) at plane $\alpha = 180°$; (b) comparison of normalized $\sqrt{\overline{v'v'}}$ component of turbulence intensity of circular uniform pier run (UPSH) with the circular compound pier runs (NUPSH 1, NUPSH 2, and NUPSH 3) at plane $\alpha = 180°$; (c) comparison of normalized $\sqrt{\overline{w'w'}}$ component of turbulence intensity of circular uniform pier run (UPSH) with the circular compound pier runs (NUPSH 1, NUPSH 2, and NUPSH 3) at plane $\alpha = 180°$

with the circular uniform pier, except at the level of the top surface of footing.

In the plane at $\alpha = 90°$ (see Kumar 2010), a small size of vortex with diminishing strength was observed near the bed of the scour hole in all the experimental runs. Similar diminishing vortical flow was also reported by Dey and Raikar (2007) for the uniform circular pier.

Fig. 10 represents the variation of size of the principal vortex at the upstream nose of the pier, with the measured scour depth for the present data and uniform circular pier data of Melville (1975), Graf and Istiarto (2002), and Dey and Raikar (2007). The size of the principal vortex varies linearly with the scour depth. Therefore, it is emphasized that the size of the principal vortex governs the scour depth at the pier nose (Kothyari et al. 1992). Linear variation,

426 / JOURNAL OF HYDRAULIC ENGINEERING © ASCE / MAY 2012

J. Hydraul. Eng., 2012, 138(5): 420-429
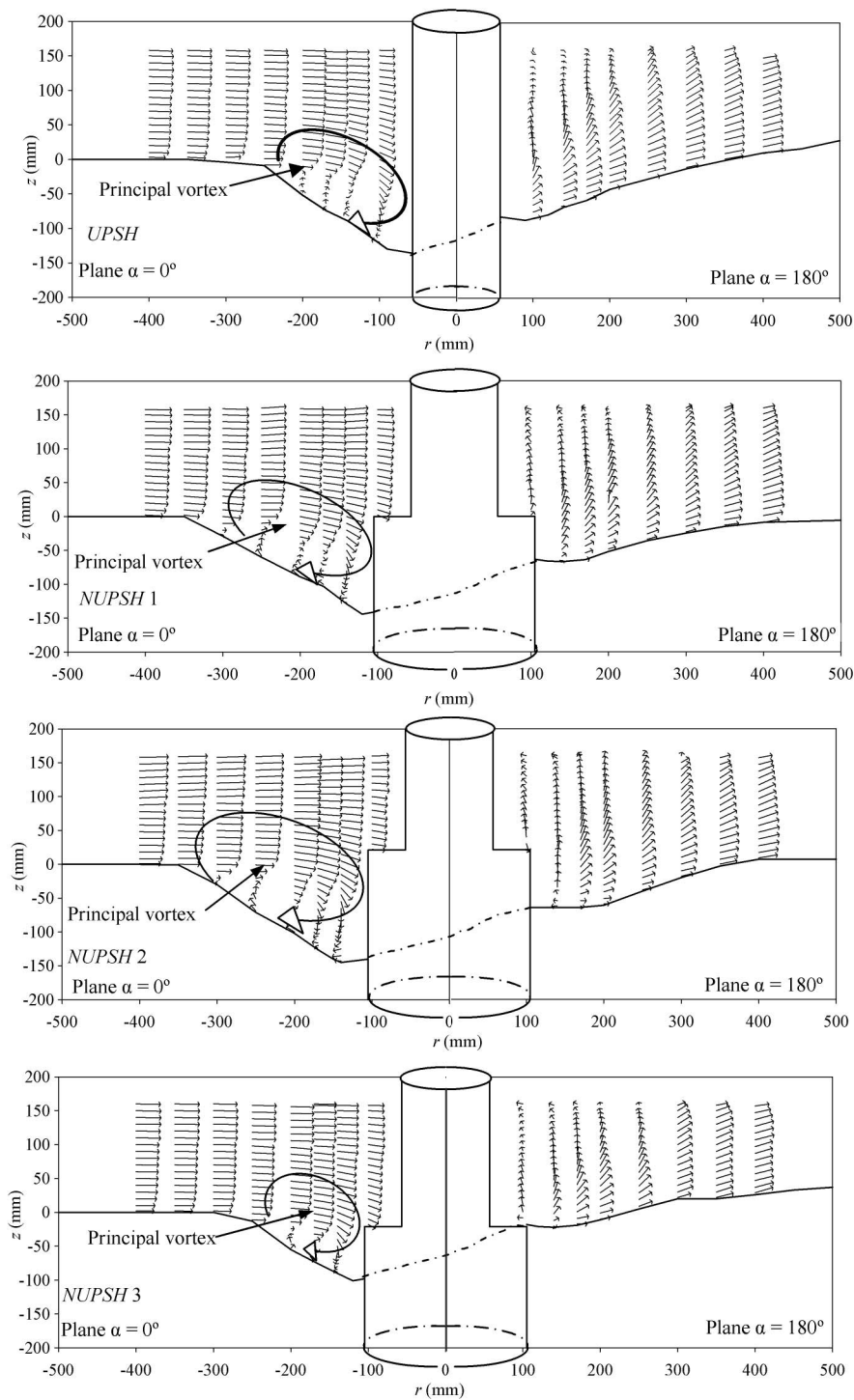
Fig. 9. Measured velocity field in the scoured area in the plane upstream and downstream of circular and compound piers

as seen in Fig. 10, also indicates that geometries of scour holes were similar for the data of different investigators.

Bed Shear Stress around the Circular Uniform Pier and Circular Compound Pier

The bed shear stress around the piers was derived for all the experimental runs. Calculations for bed shear stress were carried out by the method proposed by Wu and Rajaratnam (2000) based

on velocity measurements. On the basis of the velocities u and w measured at a distance $z \approx 4$ mm above the bed level, the velocities parallel to the bed slope of the scour hole were determined. These velocities were used to estimate the bed shear stress along the bed of the scour hole. The bed shear stress τ_b calculated by this method is normalized with bed shear stress in the approach flow τ_u.

Fig. 11 depicts the bed shear stress for all the runs at radial vertical planes $\alpha = 0°$ and 180°. In the scoured region, the bed shear stress is greatly reduced compared with the bed shear stress in the approach flow as is evident in Fig. 11. At the radial vertical plane

JOURNAL OF HYDRAULIC ENGINEERING © ASCE / MAY 2012 / **427**

J. Hydraul. Eng., 2012, 138(5): 420-429
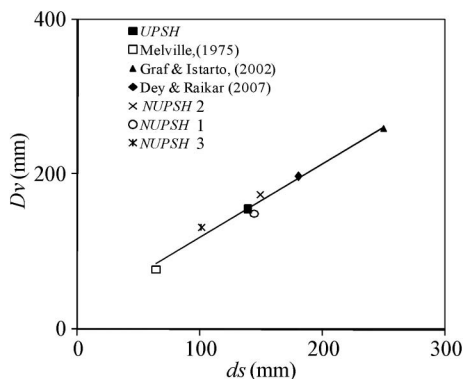
Fig. 10. Variation of observed principal vortex with depth of scour
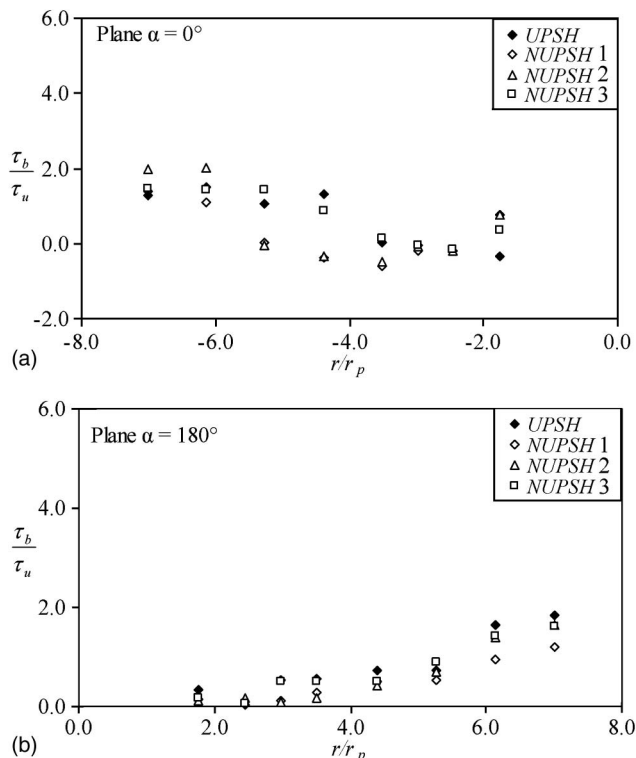
Fig. 11. Observed bed shear stress for runs UPSH, NUPSH 1, NUPSH 2, and NUPSH 3 at planes $\alpha = 0°$ and $180°$

with $\alpha = 0°$, for run UPSH in the scoured region for $r/r_p < 4.39$, the ratio τ_b/τ_u was noticed to vary from -0.353 to 0.040. The negative sign represents the reversal of flow at bed level within the scoured area. Measurement of bed shear stress in the scoured area around the circular uniform pier by Melville (1975), Ahmed and Rajaratnam (1998), Graf and Istiarto (2002) and Dey and Raikar, (2007) also showed a similar tendency of decreasing shear stress at plane $\alpha = 0°$. A trend similar to the above was noticed for compound pier runs at radial vertical plane at $\alpha = 0°$ as the ratio τ_b/τ_u here varied between -0.206 and -0.378 for run NUPSH 1; between -0.211 and -0.032 for run NUPSH 2; and between -0.167 and -0.155 for run NUPSH 3. In the plane at $\alpha = 90°$ (see Kumar 2010) the ratio τ_b/τ_u had a value less than unity. Far away from the scoured region, however, τ_b/τ_u showed

more than unity for all the runs. This observation is explained subsequently.

The data on Fig. 11(a) show that the shear stress ratio at the upstream end of the scour hole can be as high as 2.0, whereas u_*/u_{*c} on the undisturbed approach bed was equal to 0.92. The scour hole extended to more than about six times the pier radius (for example, in run NUPSH 3, also see Fig. 2). The extent of the scour hole on the upstream pier was large enough so that it was easier for flow to dive into the scour hole rather than to diverge out of the pier (Ahmed and Rajaratnam 1998). Thus, in the presence of scour hole, flow upstream pier accelerates toward the scour hole as a consequence ratio of shear stress larger than unity, which is observed in this study and in previous studies (Melville 1975; Ahmed and Rajaratnam 1998; Graf and Istiarto 2002).

In compound pier runs, $\tau_b > \tau_u$ near the top surface of the footings where scouring was not possible. In the plane at $\alpha = 90°$, $\tau_b/\tau_u = 2.37$ for run NUPSH 1, 3.42 for run NUPSH 2, and 2.5 for run NUPSH 3. In the vertical plane at $\alpha = 180°$, the ratio τ_b/τ_u had value less than unity for $r/r_p \leq 5.26$ but $\tau_b/\tau_u > 1.0$ for $r/r_p > 5.26$ for all the runs. As mentioned previously, the bed around the pier was stabilized before taking measurements with ADV. This is the reason that further scour did not occur at locations where $\tau_b/\tau_u > 1.0$. Also at $\alpha = 180°$, $\tau_b/\tau_u = 0.13$ for run NUPSH 1, 0.11 for run NUPSH 2, and 0.17 for run NUPSH 3 at the levels of the top surface of footing, whereas $\tau_b/\tau_u = 0.34$ for run UPSH at the same radial distance from the pier.

The quantification of bed shear stress within the scoured area around compound piers as presented here will be useful in developing new methods for computation of temporal variation of scour depth around compound piers.

Conclusions

Well controlled measurements were taken, using an ADV, on the flow characteristics around circular uniform piers and circular compound piers in the presence of developing (transient stage) scour holes. The present study mainly focused on quantifying the alterations caused in the flow field by changing the position of the top surface of the footing with respect to the general bed level of the channel. The followings features related to the flow field around the circular piers were noted:

1. The measurements of velocity, turbulence intensities, and Reynolds shear stress made around each of the pier models at different vertical planes exhibit almost similar profiles along the flow depth. However, the measurements close to the pier (at $r/r_p = 1.75$) revealed that a significant change occurs in the vertical profile of the flow parameters when position of the top surface of the footing varied with respect to general bed level of the channel.

2. The measured velocity data are useful for quantifying the variation in the size of principal vortex forming at the upstream nose of the pier. Because of larger exposure of the footing to the flow, the size of the principal vortex in run NUPSH 2 was 11% larger than that for run UPSH. For run NUPSH 3, the size of the principal vortex was 0.85 times that for run UPSH. The smaller vortex size in run NUPSH 3 is attributed to the vortex supporting ability of the footing top surface. The vortex supporting capability of the top surface of the footing also results in a smaller value of scour depth at the upstream nose of the pier in such scenarios (Melville and Raudkivi 1996).

3. In the wake region, flow reversal was observed in all the runs; however, the u component was higher in magnitude for UPSH runs compared with NUPSH runs. Magnitude of intensity of

turbulence is in a decreasing order, respectively, for runs NUPSH 2, NUPSH 1, UPSH, and NUPSH 3.

4. The observations made in the upstream planes revealed that, within the scoured region, the bed shear stress was much smaller compared with the bed shear stress of the approach flow. However, in the case of compound pier runs over the top surface of the footing where scour is not possible, the magnitude of the shear stress was more than that observed in the corresponding approach flow.

The data presented herein can serve as the base results when flow simulation models need to be tested. These results are also useful in modeling the scour process and developing new measures for protection against scour around piers.

Notation

The following symbols are used in this paper:

b = diameter or width of bridge pier;
b_* = diameter or width of the foundation;
d_{50} = median sediment grain diameter;
d_s = maximum scour depth below the original bed level;
d_{se} = equilibrium scour depth below the original bed level;
d_{st} = depth of scour below the initial bed level at time t;
h = depth of flow;
k = turbulent kinetic energy;
Q = discharge;
r, α, z = cylindrical coordinates in the longitudinal, transverse and vertical directions respectively;
r_p = radius of pier;
t = time after beginning of scour when scour depth is d_{st};
u, v, w = Cartesian velocity components in x, y, and z directions, respectively;
u', v', w' = fluctuation of u, v, and w components of velocity, respectively;
u_r, u_α, w = radial, angular, and vertical velocity components along the cylindrical coordinates (r, α, z);
u_* = bed shear velocity of approach flow;
u_{*c} = critical bed shear velocity for d_{50} size, defined by Shields' function;
$\sqrt{\overline{u'u'}}, \sqrt{\overline{v'v'}}, \sqrt{\overline{w'w'}}$ = longitudinal, transverse, and vertical components of turbulence intensity;
$\overline{u'w'}, \overline{v'w'}$ = components of Reynolds shear stress;
U_∞ = velocity of approach flow;
Y = depth of the top of the foundation below the initial bed level;
τ_b = shear stress at bed; and
τ_u = shear stress of the approach flow.

References

Ahmed, F., and Rajaratnam, N. (1998). "Flow around bridge piers." *J. Hydraul. Eng.*, 124(3), 288–300.

Ali, K. H. M., Karim, O. A., and O'Connor, B. A. (1997). "Flow patterns around bridge piers and offshore structures." *Proc., Theme A: Water for a Changing Global Community*, ASCE, New York, 208–213.

Dey, S., and Barbhuiya, A. K. (2005). "Flow field at a vertical–wall abutment." *J. Hydraul. Eng.*, 131(12), 1126–1135.

Dey, S., Bose, S. K., and Sastry, G. L. V. (1995). "Clear water scour at circular piers: A model." *J. Hydraul. Eng.*, 121(12), 869–876.

Dey, S., and Raikar, R. V. (2007). "Characteristics of horseshoe vortex in developing scour holes at piers." *J. Hydraul. Eng.*, 133(4), 399–413.

Graf, W. H., and Istiarto, I. (2002). "Flow pattern in the scour hole around a cylinder." *J. Hydraul. Res.*, 40(1), 13–20.

Kothyari, U. C., Garde, R. J., and Raju Ranga, K. G. (1992). "Temporal variation of scour around circular bridge piers." *J. Hydraul. Eng.*, 118(8), 1091–1106.

Kothyari, U. C., Hager, W. H., and Oliveto, G. (2007). "Generalized approach for clear-water scour at bridge foundation elements." *J. Hydraul. Eng.*, 133(11), 1229–1240.

Kumar, A. (2007). "Scour around circular compound bridge piers." Ph.D. thesis, Dept. of Civil Engineering, Indian Institute of Tech., Roorkee, India.

Kumar, A. (2010). "Experimental data of flow characteristics around the circular uniform and compound bridge piers using acoustic Doppler velocimeter." ⟨http://www.juit.ac.in/Department/civil/Ashish_Experimental_Data.pdf⟩ (Mar. 17, 2012).

Melville, B. W. (1975). "Local scour at bridge sites." *Report No. 117*, School of Engineering, Univ. of Auckland, Auckland, New Zealand.

Melville, B. W., and Chiew, Y. M. (1999). "Time scale for local scour at bridge piers." *J. Hydraul. Eng.*, 125(1), 59–65.

Melville, B. W., and Raudkivi, A. J. (1977). "Flow characteristics in local scour at bridge sites." *J. Hydraul. Res.*, 15(4), 373–380.

Melville, B. W., and Raudkivi, A. J. (1996). "Effect of foundation geometry on bridge pier scour." *J. Hydraul. Eng.*, 122(4), 203–209.

Muzzammil, M., and Gangadhariah, T. (2003). "The mean characteristics of horseshoe vortex at a cylinder pier." *J. Hydraul. Res.*, 41(3), 285–297.

Olsen, N. R. B., and Kjellesvig, H. M. (1998). "Three-dimensional numerical flow modeling for estimation of maximum local scour depth." *J. Hydraul. Res.*, 36(4), 579–590.

Richardson, J. E., and Panchang, G. P. (1998). "Three-dimensional simulation of scour-inducing flow at bridge piers." *J. Hydraul. Eng.*, 124(5), 530–540.

Salaheldin, T. M., Imran, J., and Chaudhry, M. H. (2004). "Numerical modeling of three-dimensional flow field around circular piers." *J. Hydraul. Eng.*, 130(2), 91–99.

Wahl, T. L. (2000). "WinADV computer." Bureau of Reclamation, Water Resources Research laboratory. ⟨www.usbr.gov/pmts/hydraulics lab/twah/winadv/⟩ (Aug. 10, 2011).

Wu, S., and Rajaratnam, N. (2000). "A simple method for measuring shear stress on rough boundaries." *J. Hydraul. Res.*, 38(5), 399–400.

JOURNAL OF HYDRAULIC ENGINEERING © ASCE / MAY 2012 / **429**

J. Hydraul. Eng., 2012, 138(5): 420-429